Hindawi
Journal of Applied Mathematics
Volume 2021, Article ID 7386215, 8 pages
https://doi.org/10.1155/2021/7386215

Research Article

Analytical Solution of Heat Conduction from Turbulence with an Isotropic Example

Steven A. E. Miller

University of Florida, USA

Correspondence should be addressed to Steven A. E. Miller; saem@ufl.edu

Received 26 April 2021; Accepted 26 June 2021; Published 9 July 2021

Academic Editor: Qiankun Song

Aerodynamic heating due to turbulence significantly affects the operation of high-speed vehicles and the entrainment of fluid by turbulent plumes. In this paper, the heat generated and convected by fluid turbulence is examined by rearranging the Navier-Stokes equations into a single equation for the fluctuating dependent variables external to unsteady chaotic motions. This equation is similar to the nonhomogeneous heat equation where sources are terms resulting from this rearrangement. Mean and fluctuating quantities are introduced, and under certain circumstances, a heat equation for the fluctuating density results with corresponding mean and fluctuating source terms. The resultant equation is similar to Lighthill's acoustic analogy and is a "heat analogy." A solution is obtained with the use of Green's function as long as the observer is located outside the region of chaotic motion. Predictions for the power spectrum are shown for high Reynolds number isotropic turbulence. The power spectrum decays as the inverse of the wavenumber of the turbulent velocity fluctuations. The developed theory can easily be applied to other turbulent flows if the statistics of unsteady motion can be estimated.

1. Introduction

Turbulence is the predominant state of fluid flow in most engineering applications as well as many naturally occurring physical and biological phenomena. When the intensity or convection velocity of the turbulent flow is high, then significant aerodynamic heating occurs upon the surrounding environment. This process is observed when examining the aerodynamic heating upon high-speed aircraft or the heating of the entrained fluid surrounding a turbulent jet plume. Turbulence also contributes to the aft heating of vehicles or meteors entering the Earth's atmosphere. For example, a recent study by Park et al. [1] illustrates the aerodynamic heating behind a high-speed blunt body. Also, Dyakonov et al. [2] show the heating of the surrounding environment that is in part due to reaction control jets that are integral to the Mars Science Laboratory entry capsule. Figure 1 shows two numerical examples that include a reentry capsule (see Sinha et al. [3]) and a turbulent jet (see Stich et al. [4]). Numerous examples of heat transfer due to turbulent motion in a biological phenomenon are shown by Datta [5]. Often, aerodynamic heating is due to forced convection within turbulent flows that are bounded by a surface. Alternatively, in cases where the turbulence is unbounded by a solid surface such as a jet engine exhaust or partially bounded such as a boundary layer flow, aerodynamic heating of the ambient fluid also occurs. Most investigations of aerodynamic heating are concerned with the heating of solid surfaces.

2. Previous Investigations

There are numerous studies examining aerodynamic heating effects upon flight vehicles. There are very limited studies examining heating of the ambient environment from the same turbulent flow. Due to the complex nature of turbulence, the newly developed theory is demonstrated using the simplifying assumptions of isotropy. A number of investigators have examined the temperature fluctuations of isotropic turbulence. Kovasznay [6] examined the energy spectrum of isotropic turbulence. He noted that the energy spectrum is highly dependent on the kinematic viscosity and the dissipation per unit mass. Corrsin [7] examined the decay of isotropic temperature fluctuations within isotropic turbulence with the assumption that the temperature

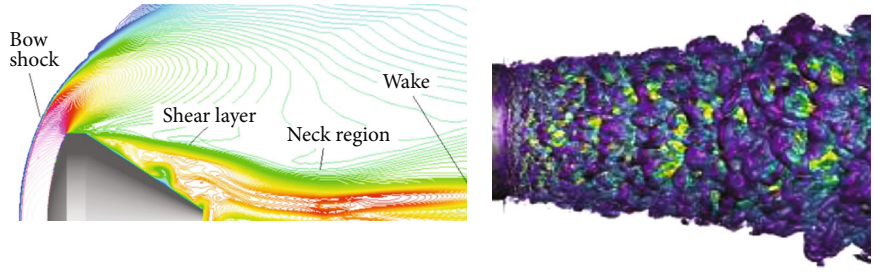

(a) (b)

Figure 1: Example applications include (a) reentry capsule aerodynamic heating [3] and (b) heating of fluid by a turbulent jet flow [4].

fluctuations do not alter the dynamics of the turbulent field. It was shown that the triple correlations of the temperature fluctuations are zero. Corrsin [8] derived the fluctuating temperature power spectrum and compared it with the velocity spectrum of isotropic turbulence. Corrsin [9] also examined the heat transfer within statistical isotropic turbulence and utilized the assumption that the temperature gradients are small and do not significantly affect the flow. Expressions for the heat transfer coefficient and correlation coefficient of the temperature fluctuations were formulated, and their dependence on the field variables was shown. Dunn and Reid [10], like Corrsin [7], examined the heat transfer within isotropic turbulence with constant temperature gradients in their final period of decay.

They found that the magnitude of heat transfer is proportional to the mean temperature gradients within the turbulent field. The Prandtl number was found to only have an effect on heat transfer when it is small. Libby and Scragg [11] examined the heating from a line source within a turbulent field downstream of a grid and predicted the heat transfer within the field. This study illustrated heat transfer effects without a bounding surface. Traci and Wilcox [12] examined the heat transfer from convecting turbulence at a stagnation point. Hyde et al. [13] and Ko and Liu [14] examined the aerodynamic heating and cooling, respectively, due to turbulence convecting over surfaces from wall jets. In both these later studies, the entrained fluid and bounding surface are under the effects of heat transfer. Very recently, de Marinis et al. [15] examined the temperature variance spectrum within isotropic turbulent fields containing a term specifically for heat production. They observed that the power spectrum with respect to wavenumber varies as $k^{-7/3}$, where k is the turbulent kinetic energy, for very diffusive fluids. Balakrishnan et al. [16] performed a direct numerical simulation of the heating from a high Reynolds number diffusive flame. A number of recent studies have used either experimental or computational techniques [17–21] and analytical techniques [22]. Investigations of heat transfer and the fluctuations due to high-intensity turbulence are usually restricted to the region within the turbulent field or surrounding solid bodies.

3. Present Approach

In this paper, we examine the aerodynamic heating of the fluid that surrounds high-intensity turbulence. We formulate an exact closed-form equation to quantify the aerodynamic heating effect due to high-intensity turbulence. The Navier-Stokes equations are rearranged into a heat conduction operator equated to the equivalent source of aerodynamic heating. This approach is similar to that of Lighthill [23] who rearranged the equations of motion and predicted the acoustic intensity due to turbulent fluid motion. The sources consist of various operations involving the spatial and temporal varying dependent variables of the Navier-Stokes equations.

Evaluation of the developed closed-form equation requires knowledge of the time and spatially dependent variables of the Navier-Stokes equations. Solutions of the Navier-Stokes equations for even the simplest flows are unavailable or difficult to obtain even with powerful computers. However, statistical quantities of simplified turbulent flows are predictable. One such case is isotropic turbulence. To demonstrate the developed theory, we examine the spectral density of fluctuating quantities outside the region of turbulent motion and model the statistical quantities using the theory of isotropic turbulence. This example is similar to that of Proudman [24] who used well-known models of two-point cross-correlations of velocity fluctuations within isotropic turbulence to predict the resultant acoustic intensity.

Next, a physical description of the problem is shown along with the development of an equation for the fluctuating far-field density. We then demonstrate the methodology by using well-known models of isotropic turbulence statistics. Finally, we summarize the aerodynamic heating upon the surrounding fluid as a function of wavenumber and turbulent kinetic energy.

4. A Finite Region of Isotropic Turbulence in an Infinite Space

Heat conduction due to turbulent motion is examined in an infinite space of three dimensions containing an ideal compressible fluid. A finite region of the domain contains fluid that is in turbulent motion and moves with a constant mean velocity through space. The external region that is not in turbulent motion only experiences fluctuations due to heat transfer and acoustic waves. These disturbances are independent and can be summed linearly. The properties of the turbulent region are statistically stationary, homogeneous, and isotropic. For this particular investigation, the turbulence is assumed to be bounded in a cube and the boundaries of the fluid with the property of isotropic turbulence are assumed to be moving with the same mean velocity as the turbulence.

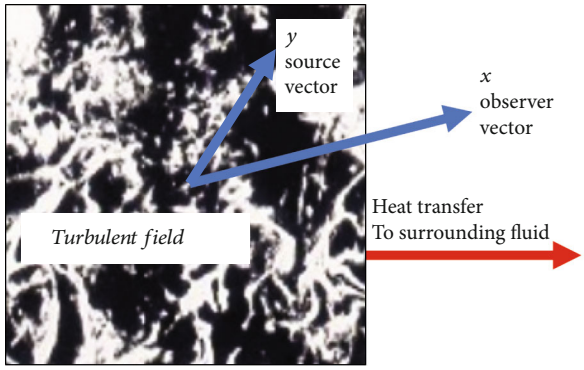

Figure 2: Homogeneous isotropic turbulence generated by a grid within a domain with source and observer vectors.

The boundary only acts to separate a finite region with the properties of fully turbulent flow and the infinite region disturbed by the perturbations due to heat transfer. The equations of motion are valid through the entire domain including the boundary. The actions of the natural evolution of isotropic turbulence cause the surrounding fluid to experience aerodynamic heating in all directions. Figure 2 shows one example of isotropic homogeneous turbulence, which heats the surrounding environment. The turbulence is photographed with a camera, and the turbulence is a smoky airflow moving through a coarse screen.

Heat that is the result of the viscous conversion of kinetic energy within the fluid is radiated into the ambient environment. The effect of aerodynamic heating on the evolution of the small and finite turbulent part of the fluid field is considered small and in thermal equilibrium. Turbulence within the source region is incompressible though the fluid is compressible. The Reynolds number based on the velocity fluctuations is large relative to the turbulent Mach number and mean velocity of the source. The entire flow field is in thermal equilibrium. Using these assumptions, which are reasonable for fully developed turbulence in both numerical and theoretical studies and in some select natural experimental instances, the properties of turbulence can be found from well-known theory. The advantage of this approach, which will be apparent in the following mathematical analysis, yields insight into the aerodynamic heating of a quiescent environment by turbulent motion.

5. Mathematical Theory: The Heat Analogy

In this section, we start with the governing equations for conservation of mass and momentum of an ideal fluid and rearrange them into a single equation. The equation contains the heat conduction operator on the left-hand side with a coefficient related to the viscosity. The right-hand side contains the terms that result from the rearrangement and are considered the source of aerodynamic heating. The governing equations are the continuity equation

$$\frac{\partial \rho}{\partial t} + \frac{\partial \rho u_j}{\partial x_j} = 0, \tag{1}$$

and the momentum equation

$$\rho \frac{\partial u_i}{\partial t} + \rho u_j \frac{\partial u_i}{\partial x_j} = \frac{\partial \tau_{ij}}{\partial x_j}, \tag{2}$$

where

$$\tau_{ij} = -p\delta_{ij} + \mu\left(\frac{\partial u_i}{\partial x_j} + \frac{\partial u_j}{\partial x_i}\right) - \frac{2}{3}\mu \frac{\partial u_k}{\partial x_k}\delta_{ij}, \tag{3}$$

where t is the time, u is the velocity vector, μ is the viscosity, ρ is the density, and δ_{ij} is the Kronecker delta function. The subscripts represent Einstein notation where i, j, and k are the principle indexes associated with the Cartesian coordinate system. Using the chain rule of calculus, it can be shown:

$$\rho u_j \frac{\partial u_i}{\partial x_j} = \frac{\partial \rho u_i u_j}{\partial x_j} - \rho u_i \frac{\partial u_j}{\partial x_j} - u_i u_j \frac{\partial \rho}{\partial x_j}. \tag{4}$$

A convenient form of the momentum equation is created by combining equations (2) and (4),

$$\rho \frac{\partial u_i}{\partial t} + \frac{\partial \rho u_i u_j}{\partial x_j} - \rho u_i \frac{\partial u_j}{\partial x_j} - u_i u_j \frac{\partial \rho}{\partial x_j} = \frac{\partial \tau_{ij}}{\partial x_j}. \tag{5}$$

Dividing equation (5) by $u_i u_j$, taking the divergence, and multiplying by the kinematic viscosity, ν, yield

$$\nu \frac{\partial}{\partial x_i}\left(\frac{\rho}{u_i u_j}\frac{\partial u_i}{\partial t}\right) + \nu \frac{\partial}{\partial x_i}\left(\left(u_i u_j\right)^{-1}\frac{\partial \rho u_i u_j}{\partial x_j}\right) - \nu \frac{\partial}{\partial x_i}\left(\frac{\rho}{u_j}\frac{\partial u_i}{\partial x_j}\right) - \nu \frac{\partial^2 \rho}{\partial x_i \partial x_j} = \nu \frac{\partial}{\partial x_i}\left(\left(u_i u_j\right)^{-1}\frac{\partial \tau_{ij}}{\partial x_j}\right). \tag{6}$$

The continuity equation (equation (1)) and the modified form of the momentum equation (equation (6)) are combined, and the terms are rearranged:

$$\frac{\partial \rho}{\partial t} - \nu \frac{\partial^2 \rho}{\partial x_i \partial x_j} = -\frac{\partial \rho u_j}{\partial x_j} - \nu \frac{\partial}{\partial x_i}\left[\frac{\rho}{u_i u_j}\frac{\partial u_i}{\partial t} + \left(u_i u_j\right)^{-1}\frac{\partial \rho u_j u_j}{\partial x_j} - \frac{\rho}{u_j}\frac{\partial u_j}{\partial x_j} - \left(u_i u_j\right)^{-1}\frac{\partial \tau_{ij}}{\partial x_j}\right]. \tag{7}$$

The resultant vector equation is summed, and moving select left-hand side terms to the right yields

$$\frac{\partial \rho}{\partial t} - \frac{\nu}{3}\frac{\partial^2 \rho}{\partial x_j \partial x_j} = \frac{\partial \rho u_j}{\partial x_j} + \sum_{i=1}^{3}\left\{\frac{\nu}{3}\frac{\partial^2 \rho}{\partial x_i \partial x_j}\left(1-\delta_{ij}\right) - \nu\frac{\partial}{\partial x_i} \cdot \left[\frac{\rho}{3u_i u_j}\frac{\partial u_i}{\partial t} + \frac{\left(u_i u_j\right)^{-1}}{3}\frac{\partial \rho u_i u_j}{\partial x_j} - \frac{\rho}{3u_j}\frac{\partial u_j}{\partial x_j}\right] + \nu\frac{\partial}{\partial x_i}\left[\frac{\left(u_i u_j\right)^{-1}}{3}\frac{\partial \tau_{ij}}{\partial x_j}\right]\right\}. \tag{8}$$

We write the right-hand side of equation (8) as the source term Γ:

$$\frac{\partial \rho}{\partial t} - \frac{\nu}{3}\frac{\partial^2 \rho}{\partial x_j \partial x_j} = \Gamma. \tag{9}$$

Equation (9) is an exact rearrangement of the governing equations of motion of a fluid. No assumptions have been made. The left-hand side is the heat equation operator but has a dependent coefficient of the kinematic viscosity divided by three. Equation (9) is a nonlinear partial differential equation, and its general solution is not known at this time; however, under special conditions, it is possible to find an analytic solution if the right-hand side is treated as a known source.

At this point, it is important to compare equation (9) with Lighthill's [23] acoustic analogy:

$$\frac{\partial^2 \rho}{\partial t^2} - c_\infty^2 \frac{\partial^2 \rho}{\partial x_i \partial x_i} = \frac{\partial T_{ij}}{\partial x_i \partial x_j}, \tag{10}$$

where c is the speed of sound and T_{ij} is Lighthill's stress tensor. The heat analogy (equation (9)) and the acoustic analogy both have a heat equation and wave equation operator on the left-hand side. The source in the heat analogy partly contains the divergence of Γ, and the source in the acoustic analogy is the double divergence of the Lighthill stress tensor. Some assumptions must be made to obtain a solution for the fluctuating field variables due to turbulent flow. The next section will demonstrate one approach that alters equation (9) with minimal loss of accuracy and retains the benefits of a first principle model.

6. Solution of the Heat Analogy

Here, we seek a solution of equation (9) in a region outside the volume undergoing chaotic motions. We assume that the coefficient ν is constant and view equation (9) as a heat operator and a source. It can easily be shown that free-space Green's function of the heat equation in three dimensions is

$$g(x,t\,;y,\tau) = \frac{H(t-\tau)}{\left[4\pi(\nu/3)^{1/2}(t-\tau)\right]^{3/2}} \exp\left[-\frac{(x-y)^2}{4(\nu/3)^{1/2}(t-\tau)}\right], \tag{11}$$

where H is the Heaviside step function, x is the observer position, y is the source position, and τ is the retarded time. The vectors x and y are shown in Figure 2. Using $g(x,t\,;y,\tau)$ and assuming Γ is known, we can immediately form the solution of equation (9):

$$\rho(x,t) = \int_{-\infty}^{\infty}\cdots\int_{-\infty}^{\infty} g(x,t\,;y,\tau)\Gamma(y,t)\,d\tau dy, \tag{12}$$

where Γ is the right-hand side of equation (8) and '$\cdots$' represents more than three consecutive integrals. Equation (12) is valid outside the source region. If knowledge of Γ is known and is integrable over space and time for a turbulent flow, then the fluctuating density outside the flow is known, or for that matter any other field variable. Unfortunately, knowledge of Γ is nearly as difficult to obtain as the general solution of the Navier-Stokes equations. Thus, we are forced to form a solution based on the statistics of the turbulence and in turn formulate a solution that is also statistical. We change Green's function within equation (12) to be frequency dependent with the use of the inverse Fourier transform:

$$\rho(x,t) = \frac{1}{2\pi}\int_{-\infty}^{\infty}\cdots\int_{-\infty}^{\infty} g(x\,;y,w)\exp\left[iw(t-\tau)\right]\Gamma(y,t)\,dw d\tau dy, \tag{13}$$

where ω is the radial frequency. The autocorrelation of ρ is formed. The power spectral density (PSD), $S(x,\omega)$, is the Fourier transform of the autocorrelation:

$$S(x,w) = \int_{-\infty}^{\infty}\overline{\rho(x,t)\rho(x,t+\tau^*)}\exp\left[-iw\tau^*\right]d\tau^*. \tag{14}$$

This equation represents fluctuations of density due to turbulent heating within a distribution of frequency components that composes the time-domain signal (see Stoica and Moses [25] for details). Integration with respect to τ^* in equation (14) is performed using the autocorrelation of equation (13) and results in

$$S(x,w) = \frac{1}{2\pi}\int_{-\infty}^{\infty} g(x\,;y,-w)g(x\,;y+\eta,w)\times R(y,\eta,\tau)\exp \cdot\left[-ew\tau\right]d\tau d\eta dy, \tag{15}$$

where $\eta = \mathrm{z} - \mathrm{y}$ and $R(y,\eta,\tau)$ is the two-point cross-correlation of Γ. The variables y and z are two independent source vectors within the turbulent field. This approach provides an opportunity to specify two-point statistics. Green's function of the heat equation in equation (15) can be simplified with the use of equation (11). The Fourier transform of equation (11) is

$$g(x;y,w)=\frac{\exp\left[-|w||x-y|/\sqrt{2\pi}(\nu/3)^{1/4}\right]}{4\sqrt{2}\pi|x-y|(\nu/3)^{3/4}|w|}\cdot\left((\nu/3)^{1/4}|w|\cos\left[-\frac{|w||x-y|}{\sqrt{2\pi}(\nu/3)^{1/4}}\right]+i(\nu/3)^{1/4}w\sin\left[-\frac{|w||x-y|}{\sqrt{2\pi}(\nu/3)^{1/4}}\right]\right). \tag{16}$$

Examining the form of Green's function in equation (15) and assuming that x is large relative to $|\eta|$ yields a simplified equation

$$g(x;y,-w)g(x;y+\eta,w)\approx\frac{3\exp\left[-\sqrt{2/\pi}\sqrt{|w||x-y|}/(\nu/3)^{1/4}\right]}{32\pi^2|x-y|^2\nu|w|^2}. \tag{17}$$

Equation (17) controls the propagation of the energy from the source to the observer in a quiescent medium. The magnitude of the fluctuations of the field variables due to aerodynamic heating falls off as $\approx\exp[-|x|]/|x|^2$. Equation (17) is inserted into equation (15):

$$S(x,w)=\frac{3}{64\pi^3\nu|w|^2}\int_{-\infty}^{\infty}\cdots\int_{-\infty}^{\infty}\cdot\frac{\exp\left[-\sqrt{2/\pi}\sqrt{|w|}|x-y|/(\nu/3)^{1/4}\right]}{|x-y|^2}R(y,\eta,\tau)\exp\cdot[-i\omega\tau]d\tau d\eta dy. \tag{18}$$

A statistical model of $R(y,\eta,\tau)$ is required to evaluate the model. To do this, we reexamine Γ with the view of isotropic turbulence. The stress tensor τ_{ij} is the term that is primarily responsible for heat generation from isotropic turbulence, and the other terms of Γ are small in comparison and are disregarded. Examining τ_{ij} in Γ and expanding

$$\frac{\partial}{\partial x_i}\left(\frac{\mu}{3\rho u_i u_j}\frac{\partial\tau_{ij}}{\partial x_j}\right)=\frac{\partial}{\partial x_i}\left(\frac{\mu}{3\rho u_i u_j}\right)\frac{\partial\tau_{ij}}{\partial x_j}+\frac{\mu}{3\rho u_i u_j}\frac{\partial^2\tau_{ij}}{\partial x_i\partial x_j}, \tag{19}$$

note that the summation is dropped and subscript i implies summation from one to three. We choose to write each dependent variable as an ensemble averaged component and a fluctuating component, $q=\bar{q}+q'$, where q represents an independent variable, the overline represents the ensemble average, and the prime denotes a fluctuating quantity. We assume that $\bar{u}_i$ is positive. Averaging equation (19) and retaining the dominant term result in

$$\Gamma\approx\frac{2\mu^2(1-\delta_{ij})}{3\bar{\rho}\bar{u}_i\bar{u}_j}\frac{\partial^3 u_j'}{\partial x_i\partial x_j\partial x_j}. \tag{20}$$

Note that derivatives of the averaged quantities are zero. We now construct the two-point cross-correlation of Γ:

$$R(y,\eta,\tau)\approx\frac{4}{9}\frac{\mu^4(1-\delta_{ij})(1-\delta_{lm})}{\bar{\rho}^2\bar{u}_i\bar{u}_j\bar{u}_l\bar{u}_m}\frac{\partial^3\overline{u_j'u_m'}}{\partial x_i\partial x_j\partial x_j}, \tag{21}$$

and a model is required for $\overline{u_j'(y,t)u_m'(y+\eta,t+\tau)}$ that satisfies an isotropic turbulent flow. It is well known that for isotropic turbulence,

$$\overline{u_j'u_m'}=\frac{1}{3}\overline{q^2}\delta_{jm}, \tag{22}$$

where $\overline{q^2}$ is the trace of the Reynolds stress tensor. The turbulent kinetic energy is

$$k=\frac{1}{2}\left(\overline{u_j'u_j'}\right)=\frac{1}{2}\overline{q^2}. \tag{23}$$

The Reynolds number relation with L is

$$\mathrm{Re}_L=\frac{\bar{\rho}k^{1/2}L}{\mu}, \tag{24}$$

where Re_L is the Reynolds number based on the integral scale of turbulence L. A simple model for the Reynolds stress within an isotropic turbulent field is

$$\overline{u_j'(y,t)u_m'(y+\eta,t+\tau)}=\frac{2}{3}\left(\frac{\mathrm{Re}_L\mu}{\bar{\rho}L}\right)^2\delta_{jm}\exp\left[-\frac{|\tau|}{\tau_s}\right]\times\exp\cdot\left[-\frac{(\xi-\tau_s\bar{u}_2)^2}{l^2}\right]\times\exp\left[-\frac{(\eta-\tau_s\bar{u}_2)^2}{l^2}\right]\exp\cdot\left[-\frac{(\zeta-\tau_s\bar{u}_3)^2}{l^2}\right], \tag{25}$$

where $l\approx L\,\mathrm{Re}^{-3/4}$ and $\tau_s\approx l/\bar{u}$. Substituting equation (25) into equation (21) yields

$$R(y,\eta,\tau)\approx\frac{8}{27}\frac{\mathrm{Re}_L^2\mu^6\delta_{jm}(1-\delta_{ij})(1-\delta_{lm})}{L^2\bar{\rho}^4\bar{u}_i\bar{u}_j\bar{u}_l\bar{u}_m}\times\frac{\partial^3\exp[-|\tau|/\tau_s]\exp\left|-(\xi-\tau_s\bar{u}_1)^2/l^2\right|\exp\left|-(\eta-\tau_s\bar{u}_2)^2/l^2\right|\exp\left|-(\zeta-\tau_s\bar{u}_3)^2/l^2\right|}{\partial x_i\partial x_j\partial x_j}. \tag{26}$$

Substituting equation (26) into equation (18) and simplifying yield

$$S(x,w)=\frac{\mathrm{Re}_L^2\mu^5\delta_{jm}(1-\delta_{ij})(1-\delta_{lm})}{72\pi^3L^2\bar{u}_i\bar{u}_j\bar{u}_l\bar{u}_m\bar{\rho}^3|w|^2}\int_{-\infty}^{\infty}\cdots\int_{-\infty}^{\infty}\frac{\exp\left[-\sqrt{2/\pi}\sqrt{|w|}|x-y|/(\nu/3)^{1/4}\right]}{|x-y|^2}\times\frac{\partial^3\exp\left[-|\tau|/\tau_s\right]\exp\left[-(\xi-\tau_s\bar{u}_1)^2/l^2\right]\exp\left[-(\eta-\tau_s\bar{u}_2)^2/l^2\right]\exp\left[-(\zeta-\tau_s\bar{u}_3)^2/l^2\right]}{\partial x_i\partial x_j\partial x_j}\exp\left[-iw\tau\right]d\tau d\eta dy. \tag{27}$$

Integrations involving τ, η, and y need to be performed. The integration with respect to τ is isolated and results in

$$\int_{-\infty}^{\infty}\exp\left[-\frac{|\tau|}{\tau_s}\right]\exp\left[-iw\tau\right]d\tau=\frac{2\tau_s}{1+\tau_s^2w^2}. \tag{28}$$

The integration with respect to η should encompass the source region. Here, we choose the source region as a cubic volume with side length a. The statistics of turbulence are independent of y. Performing the spatial integrations results in

$$S(x,w)=\frac{a^e\,\mathrm{Re}_L^2\mu^5\delta_{jm}(1-\delta_{ij})(1-\delta_{lm})}{72\pi^2L^2l^2\bar{u}_i\bar{u}_j\bar{u}_l\bar{u}_m|x|^2\bar{\rho}^3|w|^2}\frac{\tau_s}{1+\tau_s^2w^2}\exp\cdot\left[-\frac{\sqrt{2/\pi}\sqrt{|w|}|x|}{(\nu/3)^{1/4}}\right]\times\exp\left[-\frac{a^2+4\bar{u}^2\tau_s^2}{4l^2}\right]\cdot\left(\mathrm{Erf}\left[\frac{a-2\bar{u}\tau_s}{2l}\right]+\mathrm{Erf}\left[\frac{a+2\bar{u}\tau_s}{2l}\right]\right)^2\times\left(\left(a^2-2l^24\bar{u}^2\tau_s^2\right)\sinh\left[\frac{a\bar{u}\tau_s}{l_2}\right]-4a\bar{u}\tau_s\cosh\left[\frac{a\bar{u}\tau_s}{l_2}\right]\right). \tag{29}$$

Equation (29) is a closed-form equation for the PSD of density fluctuations due to aerodynamic heating from isotropic turbulence. Spectral densities of other fluid dynamic quantities such as pressure or temperature can be formulated by exactly the same methodology. Outside the source region, they are related by simple thermodynamic relations in the time domain. These later quantities are thermodynamic, and it is preferential to work with density. In the next section, equation (29) will be evaluated for a high Reynolds number isotropic turbulent flow.

7. Analysis

Equation (29) is now examined as a function of frequency. A cubic source region with lengths $a = 1$ m contains a turbulent field with turbulent kinetic energy of $k = 1 \times 10^4\ \mathrm{m^2s^{-2}}$. The integral length scale is 1/3 the cube length. The magnitude of the mean velocity is $100\ \mathrm{ms^{-1}}$, and the mean fluid density is $1.205\ \mathrm{kg\,m^{-3}}$. Viscosity of the fluid is $\mu = 1.827 \times 10^{-5}$ kg $\mathrm{m^{-1}\,s^{-1}}$. These flow properties result in an integral Reynolds number of $\mathrm{Re}_L \approx 2 \times 10^7$. Figure 3 shows the PSD of ρ per unit Strouhal number at $x = a^{-1}$. The Strouhal number, St, is the nondimensional frequency based on u and a. The PSD is adjusted by $10\log_{10}(fau^{-1})$ to conserve energy. A reference density of $\rho_{\mathrm{ref}} = 2.38 \times 10 - 10$ is selected that corresponds to the standard acoustic reference pressure for air.

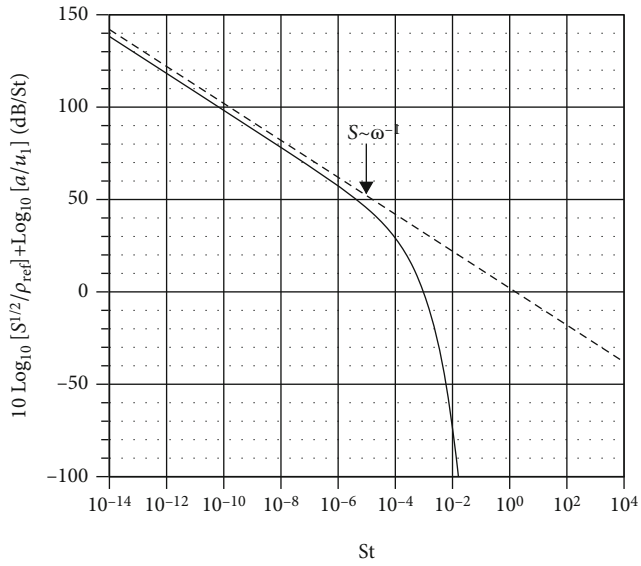

Figure 3: The power spectrum of density outside the region of isotropic turbulence at $x = 1/a$.

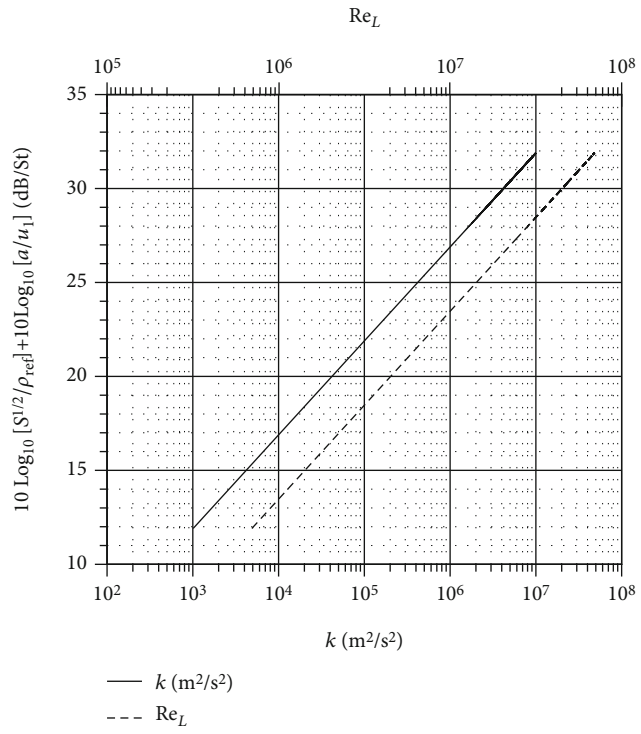

Figure 4: The power spectrum of density outside the region of isotropic turbulence at $x = 1/a$ relative to the integral Reynolds number and the turbulent kinetic energy.

The PSD of equation (29) has two distinct regions. At low- through mid-frequencies, the PSD follows a constant ω^{-1} decay. Near a Strouhal number of 10^{-5}, a transition occurs in the relation between the PSD and frequency. At high frequencies, the PSD falls off exponentially. Typically,

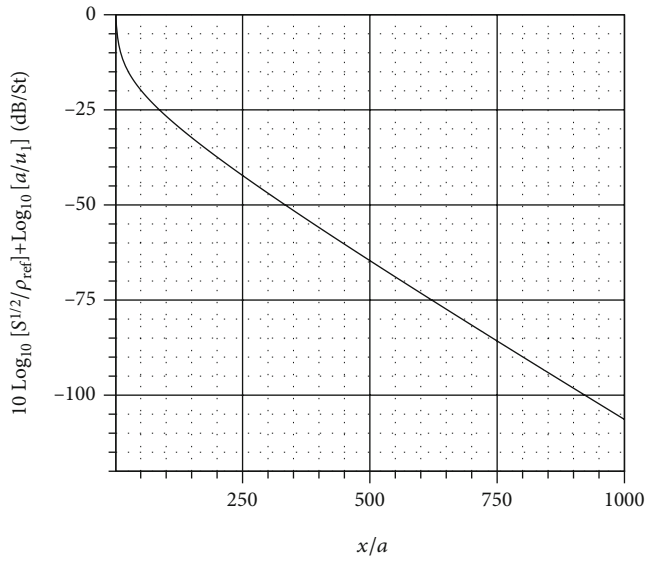

Figure 5: The power spectrum of density at 20 Hz as a function of x/a.

acoustic intensities due to turbulence occur in the range of $0.01 < \mathrm{St} < 10$ for engineering problems. At lower frequencies near the turbulent flow field, the fluctuations due to heat from isotropic turbulence dominate the fluctuations of acoustic waves.

Next, the variation of the PSD relative to Re_L and k is examined. Figure 4 shows the variation of the PSD relative to Re_L (top horizontal axis) and k (lower horizontal axis). The frequency is held constant at $f = 20$ Hz, and all other parameters remain the same. S goes as k, and Re_L increases as the square of k. This is reflected by examining the powers on the x-axis of Figure 4.

The variation of the PSD with increasing observer distance is examined in Figure 5. The observer distance is varied from $x/a = 1$ through $x/a = 1000$. As before, the frequency is $f = 20$ Hz, and the other parameters remain the same. As dictated by Green's function of the heat equation, the fall-off of the fluctuating density goes as $\approx \exp[-|x|]/|x|$. The influence of the exponential term can be seen relatively close to the source ($x/a \approx 1/2$) and not at large x/a. Relative to acoustic perturbations that fall off as $\approx x^{-1}$, the fall-off due to the heat conduction is much larger. It is not surprising that acoustic waves dominate measured signals for large x/a (compact source) for practical purposes. Also, very close to the source, it is likely that the acoustic perturbations are completely dominated by the fluctuations due to heat transfer, as evanescent waves are present.

8. Summary and Conclusion

A heat analogy that is similar to the acoustic analogy is formulated based on the Navier-Stokes equations. If the turbulent field is convecting at a constant speed, a solution can be formulated for the heat analogy with the use of Green's function of the free-space heat equation. The time-dependent variation of the field variables due to unsteady aerodynamic heating can be found if the fluctuating quantities of the source are known. A statistical solution is formulated that relates the power spectrum of the fluid density to statistical quantities of the unsteady aerodynamics. An example analysis using this statistical approach is conducted by using the theory of isotropic turbulence. This analysis shows that the energy due to unsteady aerodynamic heating from slowly convecting isotropic turbulence falls off from the source as $\exp[-|x|]\,|x|^{-1}$. Also, the power spectrum of the fluid density falls off with the characteristic frequency as the inverse of frequency or corresponding wavenumber. Future experimental measurements would help to validate this theoretical investigation. Applications of this theory can easily be extended to flows with high-intensity convecting turbulence that includes heated turbulent plumes, supersonic or hypersonic boundary layers, and combustion. The theory can also be used for other turbulent flows (for example, low Reynolds number flows), but the effect of heat transfer from the turbulent motions would be smaller by many orders of magnitude relative to traditional turbulent convective heat transfer flows.

Data Availability

There are no data used in this research study.

Conflicts of Interest

There are no conflicts of interest.

Acknowledgments

This work is inspired by and dedicated to the creative ideas of Sir M. James Lighthill, FRS.

References

[1] G. Park, S. L. Gai, and A. J. Neely, "Aerothermodynamics behind a blunt body at superorbital speeds," *AIAA Journal*, vol. 48, no. 8, pp. 1804–1816, 2010.

[2] A. Dyakonov, M. Schoenenberger, W. Scallion, J. V. Norman, L. Novak, and C. Tang, "Aerodynamic interference due to MSL reaction control system," in *41st AIAA Thermophysics Conference*, pp. 2009–3915, San Antonio, Texas, 2009.

[3] K. Sinha, M. Barnhardt, and G. Candler, "Detached eddy simulation of hypersonic base flows with application to fire II experiments," in *34th AIAA Fluid Dynamics Conference and Exhibit*, Portland, Oregon, June 2004.

[4] G. Stich, J. Housman, J. G. Kocheemoolayil, C. C. Kiris, J. E. Bridges, and C. A. Brown, *Hybrid RANS/LES simulation of jet surface interaction noise*, NASA Report Number ARC-E-DAA-TN68934, 2019.

[5] A. Datta, "Biological and bioenvironmental heat and mass transfer," in *Food Science and Technology*, Taylor & Francis, 2002.

[6] L. S. G. Kovasznay, "Spectrum of locally isotropic turbulence," *Journal of the Aeronautical Sciences*, vol. 15, no. 12, pp. 745–753, 1948.

[7] S. Corrsin, "The decay of isotropic temperature fluctuations in an isotropic turbulence," *Journal of the Aeronautical Sciences*, vol. 18, no. 6, pp. 417–423, 1951.

[8] S. Corrsin, "On the spectrum of isotropic temperature fluctuations in an isotropic turbulence," *Journal of Applied Physics*, vol. 22, no. 4, pp. 469–473, 1951.

[9] S. Corrsin, "Heat transfer in isotropic turbulence," *Journal of Applied Physics*, vol. 23, no. 1, pp. 113–118, 1952.

[10] D. W. Dunn and W. H. Reid, *Heat transfer in isotropic turbulence during the final period of decay*, vol. 4186, NACA Technical Note, 1958.

[11] P. A. Libby and C. A. Scragg, "Diffusion of heat from a line source downstream of a turbulence grid," *AIAA Journal*, vol. 11, no. 4, pp. 562-563, 1973.

[12] R. M. Traci and D. C. Wilcox, "Freestream turbulence effects on stagnation point heat transfer," *AIAA Journal*, vol. 13, no. 7, pp. 890–896, 1975.

[13] C. R. Hyde, B. R. Smith, J. A. Schetz, and D. A. Walker, "Turbulence measurements for heated gas slot injection in supersonic flow," *AIAA Journal*, vol. 28, no. 9, pp. 1605–1614, 1990.

[14] S. Ko and D. Y. Liu, "Experimental investigations on effectiveness, heat transfer coefficient, and turbulence of film cooling," *AIAA Journal*, vol. 18, no. 8, pp. 907–913, 1980.

[15] D. de Marinis, S. Chibbaro, M. Meldi, and P. Sagaut, "Temperature dynamics in decaying isotropic turbulence with Joule heat production," *Journal of Fluid Mechanics*, vol. 724, pp. 425–449, 2013.

[16] G. Balakrishnan, S. Sarkar, and F. Williams, "Direct numerical simulation of diffusion flames with large heat release in compressible homogeneous turbulence," in *AIAA 31st Joint Propulsion Conference and Exhibit*, San Diego, California, July 1995.

[17] R. Pecnik and A. Patel, "Scaling and modelling of turbulence in variable property channel flows," *Journal of Fluid Mechanics*, vol. 823, 2017.

[18] G. Melina, P. Bruce, G. Hewitt, and J. Vassilicos, "Heat transfer in production and decay regions of grid-generated turbulence," *International Journal of Heat and Mass Transfer*, vol. 109, pp. 537–554, 2017.

[19] J. Ahn, E. M. Sparrow, and J. M. Gorman, "Turbulence intensity effects on heat transfer and fluid-flow for a circular cylinder in crossflow," *International Journal of Heat and Mass Transfer*, vol. 113, pp. 613–621, 2017.

[20] D. L. Albernaz, M. Do-Quang, J. C. Hermanson, and G. Amberg, "Droplet deformation and heat transfer in isotropic turbulence," *Journal of Fluid Mechanics*, vol. 820, pp. 61–85, 2017.

[21] A. V. Dmitrenko, "Estimation of the critical Rayleigh number as a function of the initial turbulence of the boundary layer at a vertical heated plate," *Heat Transfer Research*, vol. 48, no. 13, pp. 1195–1202, 2017.

[22] A. V. Dmitrenko, "Analytical determination of the heat transfer coefficient for gas, liquid and liquid metal flows in the tube based on stochastic equations and equivalence of measures for continuum," *Continuum Mechanics and Thermodynamics*, vol. 29, no. 6, pp. 1197–1205, 2017.

[23] M. J. Lighthill, "On sound generated aerodynamically. I. General theory," *Proceedings of the Royal Society of London A*, vol. 211, no. 1107, pp. 564–587, 1952.

[24] I. Proudman, "The generation of noise by isotropic turbulence," *Proceedings of the Royal Society of London A*, vol. 214, no. 1116, pp. 119–132, 1952.

[25] P. Stoica and R. L. Moses, *Spectral Analysis of Signals*, Pearson Prentice Hall, Upper Saddle River New Jersey, 2005.